Pile-Group Response to Large Soil Displacements and Liquefaction: Centrifuge Experiments versus a Physically Simplified Analysis

Panagiota Tasiopoulou[1]; Nikos Gerolymos[2]; Takashi Tazoh[3]; and George Gazetas, M.ASCE[4]

Abstract: The paper presents a physically simplified method for computing displacements and structural forces on piles under conditions of lateral spreading triggered by the large seaward displacement of a harbor quay wall. The method avoids the empirical selection of stiffness-reduction factors and the associated use of *p-y* curves that current state-of-the-art methods use. Instead, the three-dimensional (3D) highly nonlinear problem is approximated in two steps, both involving two-dimensional (2D) plane-strain analyses. The first step involves a vertical (representative) slice in which the pile group has been omitted and that, shaken at its base, gives the permanent deformation of the quay wall and of the liquefiable soil. It is an effective stress analysis. In the second step, a horizontal (representative) slice taken from the middle of the liquefiable zone is subjected to an outward quay wall displacement; the goal is to evaluate the reduction of the pile displacement over the free-field one and the ensuing pile group distress. The pile resistance to ground deformation depends heavily on the constraints imposed by the superstructure, as well on the exact stiffness of the soil layers. Thus, the interplay between soil piles-quay wall under soil flow conditions is captured in a physically meaningful way. The predictions compare well with results from two centrifuge tests. **DOI: 10.1061/(ASCE)GT.1943-5606.0000759.**

CE Database subject headings: Spread foundations; Pile groups; Soil liquefaction; Soil-structure interactions; Experimentation; Displacement; Computation.

Author keywords: Lateral spreading; Pile; Quay wall; Liquefaction; Sheet-pile wall; Soil-structure interaction.

Introduction

The 1995 Hyogoken-Nambu (Kobe) earthquake provided a wide variety of foundation and quay wall failures attributed to soil liquefaction and subsequent lateral displacement of the ground. Extensive liquefaction triggered movement of quay walls about 1–4 m toward the sea, which in turn caused significant lateral spreading of the liquefied ground to distances up to 100 m from the waterfront (Yasuda 2004). The ground flow brought severe damage to many structures in the vicinity, involving deep foundations, such as piles or caissons. In the majority of case histories, the type of foundation that suffered more because of ground flow and was associated with bridge failures and building damages (Tokimatsu et al. 1996; Tokimatsu and Asaka 1998) consists of piles. Conversely, it should be noted that the existence of piles inhibited the lateral ground displacement even if this involved the depletion of their ultimate structural strength. Miyakawa bridge, illustrated in Fig. 1, presents a characteristic case where this mechanism is evident. This small bridge with a span of only 42 m is simply supported on two pile-founded abutments. The piers sustained an outward displacement of 0.5 m as a result of lateral spreading of the liquefied riverbanks while the piles suffered severe failure. However, the existence of the piles limited the lateral ground movement along the axis of the bridge, as shown by the ground deformation line along the boundary of the riverbanks. The lateral displacement of the liquefied soil in the free field was measured at about 2 m.

Numerous analytical and experimental studies have been performed since the Kobe 1995 earthquake, aiming to elaborate on the mechanism of soil-pile interaction under soil flow, triggered by extensive liquefaction, and to develop realistic design methods for the piles [Japan Road Association (JRA) 1996; Caltrans 1990]. The laterally moving soil mass carries the overlying soil and provides the driving force displacing the pile a certain distance, in function of the relative stiffness between piles and soil (Boulanger et al. 2003). The magnitude of soil movement, the lateral load of the surficial nonliquefiable soil layer, the stiffness degradation of the liquefiable zone, and the rigidity of the pile-structure system are the key parameters in a complicated interplay; they must properly be taken into account for a realistic assessment of the pile response caused by soil flow (Cubrinovski et al. 2006).

In engineering practice, several methods have been formulated to this end. In general, they can be classified into three broad categories: (1) force-based methods, which include the method of the JRA (1996), the limit equilibrium-type method (Dobry and Abdoun 2001; Dobry et al. 2003), and the viscous fluid method (Hamada 2000; Yasuda et al. 2001); (2) displacement-based methods, also

[1]Ph.D. Candidate, School of Civil Engineering, National Technical Univ. of Athens, 9 Iroon Polutechniou Str., P.C. 15780 Zografou, Athens, Greece (corresponding author). E-mail: ptasiopoulou@gmail.com

[2]Lecturer, School of Civil Engineering, National Technical Univ. of Athens, 9 Iroon Polutechniou Str., P.C. 15780 Zografou, Athens, Greece. E-mail: gerolymos@gmail.com

[3]Visiting Professor, School of Engineering, Toyama Prefectural Univ., Kurokawa 5180, Imizu, Toyama 939-0398, Japan. E-mail: tazohtakashi@gmail.com

[4]Professor, School of Civil Engineering, National Technical Univ. of Athens, 9 Iroon Polutechniou Str., P.C. 15780 Zografou, Athens, Greece. E-mail: gazetas@ath.forthnet.gr

Note. This manuscript was submitted on January 20, 2011; approved on April 25, 2012; published online on April 28, 2012. Discussion period open until July 1, 2013; separate discussions must be submitted for individual papers. This paper is part of the ***Journal of Geotechnical and Geoenvironmental Engineering***, Vol. 139, No. 2, February 1, 2013. ©ASCE, ISSN 1090-0241/2013/2-223–233/$25.00.

J. Geotech. Geoenviron. Eng. 2013.139:223-233.

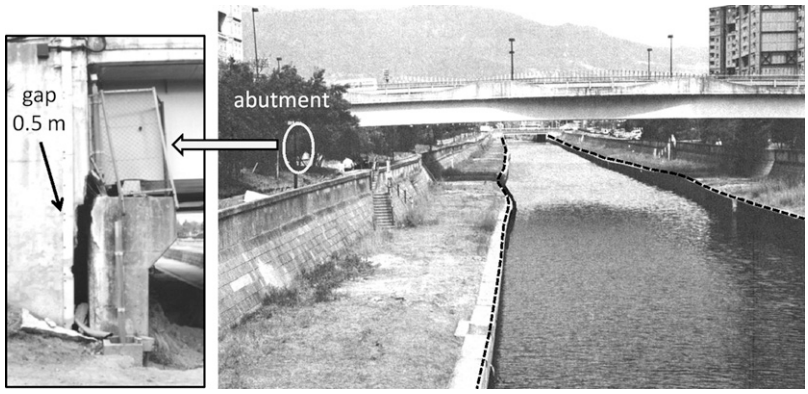

Fig. 1. Miyakawa bridge simply supported on pile-founded abutments after the Kobe earthquake in 1995: the presence of the piles limited the lateral ground movement along the bridge axis, shown with the ground deformation line along the boundary of the riverbanks (dashed line) (photographs by Professor G. Gazetas)

known as (pseudostatic) beam on nonlinear Winkler foundation methods, according to which the free field soil displacement is imposed to the pile through empirical *p-y* Winkler springs (Boulanger et al. 2003); and (3) the hybrid force-displacement methods, comprising a combination of the first two (Cubrinovski and Ishihara 2004).

These methods are mainly single pile analyses based on simplifying assumptions regarding the stiffness degradation of the liquefied soil layer and the conditions of the soil-pile interaction, such as the appropriate direction of the force exerted on the pile by the upper nonliquefiable layer. Inevitably, considerable uncertainty is hidden behind all these methods of postliquefaction analysis (Finn and Fujita 2002; Berrill and Yasuda 2002).

In this paper, a new simple physical method of analysis is presented, appropriate for all types of pile configuration (single piles, pile groups). The method falls into a hybrid displacement and force-based category and avoids the empirical selection of stiffness-reduction factors to be applied to the associated *p-y* curves. The method will be validated by satisfactorily reproducing the results of two different centrifuge experiments (Sato et al. 2001; Tazoh et al. 2005).

Description of Centrifuge Experiments Conducted at the Shimizu Institute of Technology, Tokyo

Two series of dynamic centrifuge experiments were conducted in Shimizu's Institute of Technology, Japan (Sato et al. 2001; Tazoh et al. 2005), to evaluate the seismic response of pile-foundation systems in the presence of liquefaction, large quay wall movement, and subsequent lateral spreading. All the centrifuge models were placed in a laminar box and subjected to a 30*g* acceleration field. Silicon oil, with a viscosity 30 times higher than that of water, was used for saturation of the soil deposit to achieve a single scale for both dynamic and diffusion time (Wood 2004).

Initially, Sato et al. (2001) performed two similar centrifuge tests (Centrifuge Models 1a and 1b) aiming to estimate the influence of the presence of piles behind a sheet pile quay wall in terms of soil deformation and quay wall displacement (Fig. 2). Centrifuge Model 1a contains a floating sheet pile quay wall behind a waterfront area. The backfill consists of four layers including a liquefiable layer of relatively loose sand that is 4.2 m thick, which underlies a surficial equally loose but unsaturated layer and overlies two layers of dense nonliquefiable sand. The base of the model is excited by a sinusoidal motion of 12 cycles with frequency and maximum acceleration in prototype scale, equal to 2 Hz and 0.20*g*, respectively. Centrifuge Model 1b is identical to 1a, with the only difference being that Model 1b also contains a 2×4 pile group connected with a massive footing (cap) at the top and is located 2.75 m behind the quay wall. The input motion at the base of the model remains the same as in Model 1a. Thus, the soil-pile interaction under ground flow conditions can easily be quantified by directly comparing the measured soil displacements behind the quay wall, obtained from the two centrifuge models. Pore-pressure transducers were positioned in the middle of liquefiable zone in the free field. Horizontal displacement transducers were also used to measure the quay wall movement and the distribution of surficial lateral soil displacement behind the quay wall, as shown in Fig. 2. In the case of Model 1b, a displacement transducer was also installed at the top of the footing.

Soil liquefaction occurred in the free field (Location P1) after three to four cycles of the input motion in Model 1a. The quay-wall gradually moved outward during shaking, reaching a residual value of 0.8 m at the top at the end of shaking. Lateral ground flow conditions were induced behind the quay wall from the combination of soil liquefaction in the free field and large outward movement of the quay wall. The soil displacements decreased in inverse proportion to the distance from the quay wall, as expected. In particular, the surficial soil displacement, in Model 1a, was measured 0.5 m at the end of shaking at the location to be occupied by the piles in Model 1b (2.75 m behind the quay wall). However, in the case of Model 1b, the presence of the pile group influenced significantly the ground flow by reducing the quay wall horizontal displacement at the top from 0.8 (Model 1a) to 0.45 m at the end of shaking. Moreover, the pile group residual displacement recorded atop the footing was merely 0.05 m—a 10-fold decrease from the free field (0.5 m) simulated in Model 1a. Thus, the ground flow conditions induced pile deformation, but at the same time, the pile-structure resistance limited soil movement. Both Models 1a and 1b are analyzed.

After capturing the basic effect of the pile group existence on liquefaction-induced soil flow behind the quay wall, a second series of centrifuge experiments was performed to further investigate the problem, involving a large range of key factors (Tazoh et al. 2005). All the models of this series had a similar pattern as in the first series, but they included a 2×2 pile group connected with a massive footing (cap) at the top (Fig. 2). Moreover, the input wave at the base of the models consists of a 2-Hz sinusoidal motion of 16 cycles and peak acceleration equal to 0.27*g*. It is evident that this time the input motion has a larger peak acceleration and longer duration than in the first series.

J. Geotech. Geoenviron. Eng. 2013.139:223-233.

The centrifuge experiment chosen to be analyzed from the second series corresponds to Model 2 in Fig. 2. The pile group is located 3 m behind the quay wall, and no superstructure is involved. The results of this particular test indicated that liquefaction occurred in the free field within the liquefiable zone (at Location P2 illustrated in Fig. 2). The quay wall movement was measured approximately 0.6 m at the end of shaking, whereas the footing displacement reached a maximum residual value of 0.1 m.

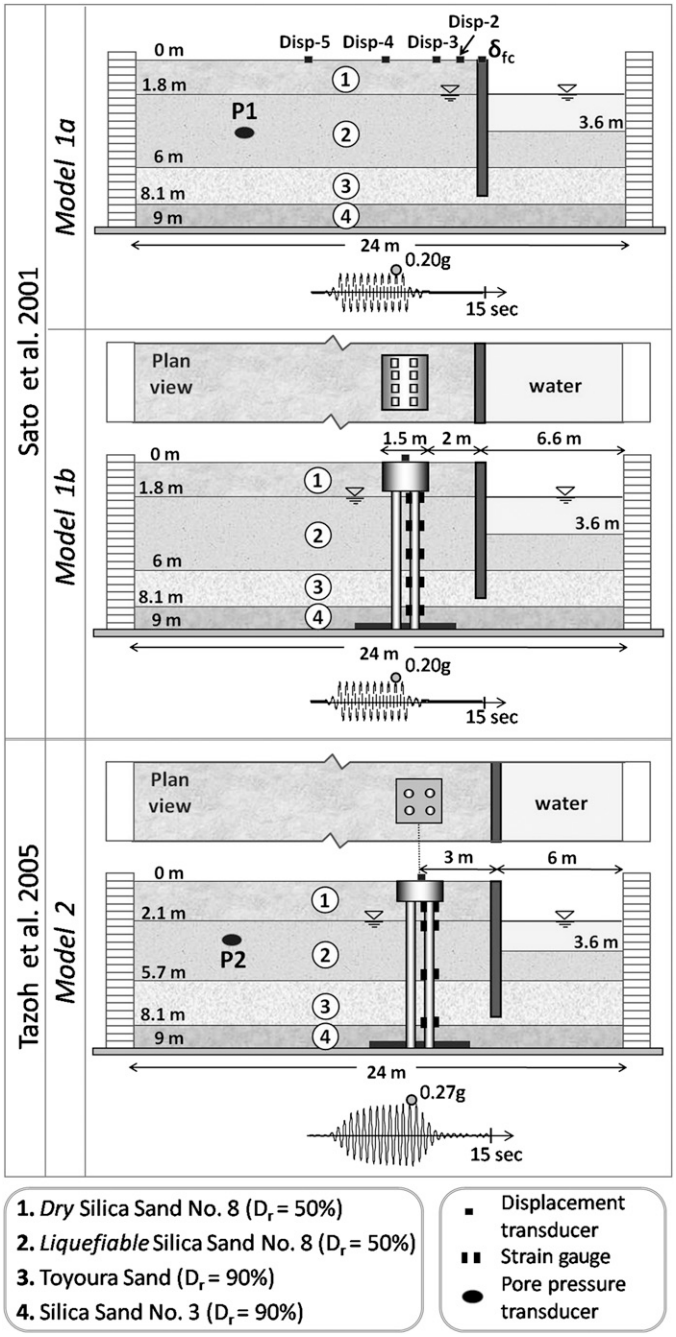

Fig. 2. Geometry and soil properties of three similar centrifuge models with a floating rigid quay wall: Model 1a (without piles); Model 1b (with 2×4 capped piles in the backfill) by Sato et al. (2001); and Model 2 (2×2 rigidly capped piles) by Tazoh et al. (2005); dimensions in prototype scale; excitations shown at the base of the models

Three-Dimensional Problem as a Combination of Two Plane Subproblems

The problem at hand is truly three-dimensional (3D) because of the presence of the pile group. The difficulty of reliably modeling the dynamic response of such a 3D geometry in the face of large soil displacements following liquefaction and outward movement of the quay wall is evident. To overcome this difficulty, a two-step approach was developed, the concept of which is shown in Fig. 3.

First Step: Two-Dimensional Dynamic Analysis of Plane Vertical Section Without Piles

The system formed with a section parallel to the x-z plane (Fig. 3), i.e., perpendicular to the quay wall, from which the piles have been omitted, will deform in plane strain when the excitation is parallel to x. Numerical discretization of a finite-difference formulation is adopted, using the code *FLAC* (Itasca Consulting Group 2005). This system is subjected to base seismic excitation, and its dynamic response is analyzed in terms of effective stresses. Pore water pressure development and dissipation are suitably taken into account. The possible onset of liquefaction and the subsequent lateral spreading that may be triggered by the possible large outward rotation and displacement of the quay wall are modeled in a realistic way. This step establishes the response of the unperturbed free field,

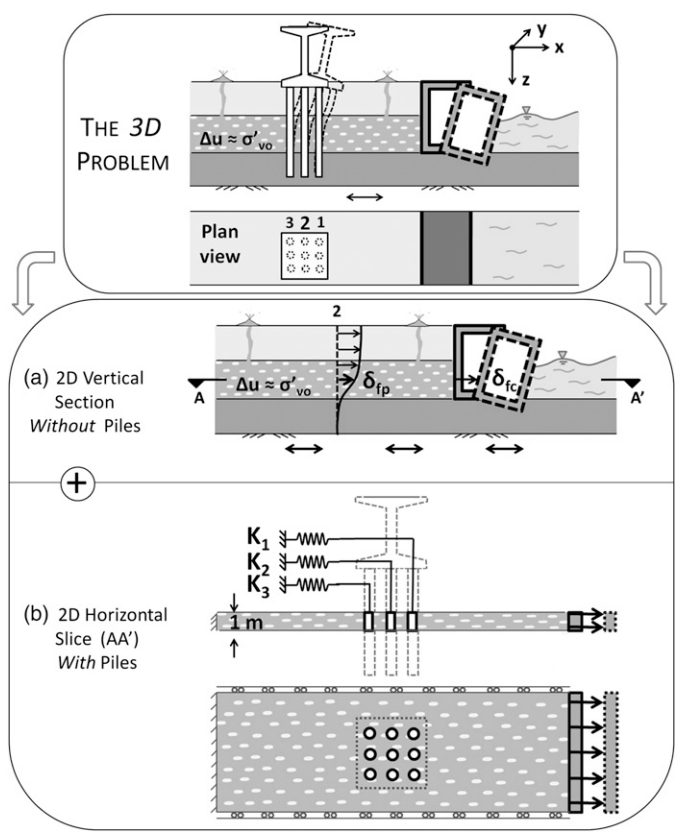

Fig. 3. Sketch of the 3D problem and its simplified decomposition into two 2D plane-strain subproblems: (a) a vertical 1-m-thick slice without the piles, subjected to the seismic base excitation, gives the caisson displacement, δ_{fc}, and the free-field movement, δ_{fp}, at the (hypothetical) location of the pile-group center; (b) a horizontal 1-m-thick slice at the middle of the liquefiable zone with the pile sections properly constrained, subjected to lateral outward displacement

J. Geotech. Geoenviron. Eng. 2013.139:223-233.

and our interest for the next step centers on (1) the quay wall displacement, (2) the displacement of the hypothetical vertical line where the center of piles will be placed, and (3) the stiffness and strength reduction of the liquefiable soil layer. Ground inclination and topographic irregularities such as riverbanks and existing structural boundaries such as quay walls in the current case, can be included in the model but not the piles. Although the dynamic numerical analysis provides the required results at all times, the residual values after the end of the shaking are of greater importance because of the accumulative nature of the liquefaction-induced soil flow.

Second Step: Two-Dimensional Static Analysis of a Horizontal Slice Containing the Piles

In the free field, inserting the group of piles will inhibit the unperturbed flow of the liquefied soil, reducing its displacements in the neighborhood of the group. In return, the piles will be subjected to soil reactions (a kinematic type of loading, in the prevailing terminology). From this step of analysis, a reduction factor is deduced, herein termed as ratio α, of the pile displacement over the free-field soil displacement (adequately away from the piles), as illustrated in Fig. 4. This ratio reflects the soil-pile interaction caused by soil flow in quantitative terms. Then, the pile displacement of the real 3D problem can be estimated by multiplying the ratio α with the actual free field soil displacement, δ_{fp}, computed from the first step of analysis.

The goal of this step of the analysis is to evaluate the reduction of the pile displacement compared with the free-field soil deformation rather than the individual values of pile and free-field soil displacement. It is the ratio of the two quantities that is of interest.

The essence (not the details) of this soil-pile interplay will be captured approximately by analyzing a horizontal unit-thickness slice of the complete system from a certain depth. This slice, parallel to the *x-y* plane, comprises not only the quay wall front and the retained soil layer at the particular depth but also the suitably restrained pile group (Fig. 3). Plane-strain conditions are assumed. Deformation of this system is triggered by pseudostatically imposing an outward displacement at the front boundary that simulates the wall. The slice can be chosen from a representative depth, e.g., from the middle of the liquefied layer, z_s (as it is chosen for this case study), or from the middle of the backfill in the case of uniform soil behind the wall. The liquefied soil layer surrounding the piles is represented by a uniform degraded shear modulus, G_L, and is assumed to behave elastically. The boundary conditions of the model are illustrated in Fig. 3(b). The lateral boundaries, which allow movement in the *x*-direction, are placed at a great distance from the pile group to achieve free-field soil conditions.

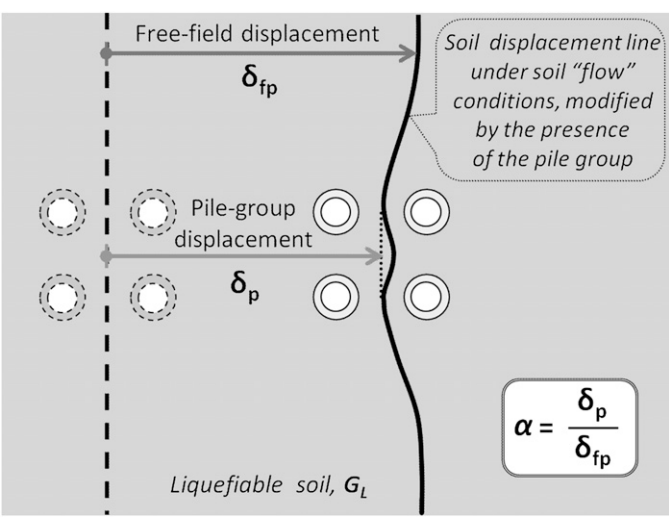

Fig. 4. Second step of analysis: definition of ratio α as the pile group displacement over the free-field soil displacement caused by liquefaction-induced soil flow (plan view)

Critical for the success of this step is the modeling of the resistance of the pile slices (inclusions) to the deforming or flowing soil. Evidently, this resistance does not derive solely from the higher modulus of elasticity of the piles–this would provide a rather insignificant resistance to soil flow. It stems from the resistance to the lateral movement of the whole pile-structure system. This resistance can be modeled through a linear (out of plane) spring resisting the movement of each pile. The computation of the modulus of such springs will be discussed later, but it is clear that, in addition to the pile dimensions, its fixity (or not) at the base of the soil layer, the pile cap connection, and the superstructure kinematic constraints are of great importance. For a rigidly capped pile group, as in the particular centrifuge examples, a single spring for the whole group may be considered.

In addition to the appropriate simulation of the pile group configuration, interface elements were used in the perimeter of the pile sections. The soil-pile interface is assumed to be smooth, allowing the surrounding soil to flow around the piles. Moreover, to avoid dragging forces being exerted on the front half of the pile slice, tension cutoff was assigned to the interface elements.

Once the elastic pseudostatic analysis was conducted, both the pile group and the free-field soil displacements are recorded. The free-field soil displacement is measured at a distance from the front boundary equal to that of the center of the pile group, as shown in Fig. 4. The pile group displacement divided by the free-field soil movement gives the ratio α.

It is evident that the effectiveness of the numerical analysis of the horizontal slice, and thus the appropriate estimation of ratio α at the mid-depth, z_s, depends on the proper selection of the horizontal stiffness of each pile section, K, and the shear modulus of the liquefiable soil layer, G_L.

Horizontal Stiffness, *K*, of Each Pile Section

Every single pile of the pile group can be simulated as a vertical beam element with appropriate kinematic constraints at the boundaries (boundary conditions). The rotation at the top depends on the fixity of the pile cap, i.e., on the number of piles and their axial stiffness. Increasing any one of these two parameters tends to restrain the rotation at the pile head.

The active length of the pile depends on the depth to fixity below the liquefied layer. In the literature, this depth is obtained from the length of an equivalent column fixed at its base and having the same stiffness as the pile, thereby producing the same displacement under lateral load. Depth to fixity values can be estimated from available dimensionless charts provided by several researchers (Priestley et al. 1996; Budek et al. 2000; Caltrans 1990). In general, the depth to fixity is measured from the ground surface. However, in the current case of liquefaction-induced soil flow where the liquefied soil cannot provide significant support to the piles (while flowing around them), the depth to fixity can be measured from the end of the liquefied zone. Therefore, the active length of the pile column can be estimated by adding the depth to fixity to the portion of the pile embedded in the liquefied zone and its overlying layers.

In retrospect, every single pile is equivalent to a column of a certain length fixed at the bottom with a certain degree of rotational freedom at the top. The pile slice in the numerical model is just a section at the mid-depth of the liquefied layer. Thus, the horizontal

J. Geotech. Geoenviron. Eng. 2013.139:223-233.

stiffness, K (kN/m), of each pile section is defined as the point load that must be exerted on the pile column at that depth to cause a unit displacement at the same depth (Fig. 5).

Shear Modulus, G_L, of the Liquefiable Soil

In the framework of a simplified analysis of the horizontal slice, an equivalent shear modulus of the liquefiable soil can be estimated by the following equation:

$$G_L = \int_0^{H_L} \frac{\tau(z)}{\gamma(z)} dz \tag{1}$$

where, H_L = thickness of the liquefiable zone, τ = residual shear stress, and γ = accumulated shear strain at the end of shaking, obtained from the numerical analysis of the free field (Step 1). This is how the stiffness degradation of the soil caused by liquefaction is taken into account.

Herein, three sets of elastic pseudostatic analyses of the horizontal slice were conducted by parametrically changing the values of K and G_L for three different pile configurations: a single pile; a 2×2 pile group (Tazoh et al. 2005); and a 2×4 pile group (Sato et al. 2001).

The ratio α is shown to be sensitive only to the relative stiffness between the pile and the liquefied soil, K/G_L (m), and thus, it is obtained as a function of the ratio K/G_L, shown in Fig. 6 for the three pile configurations.

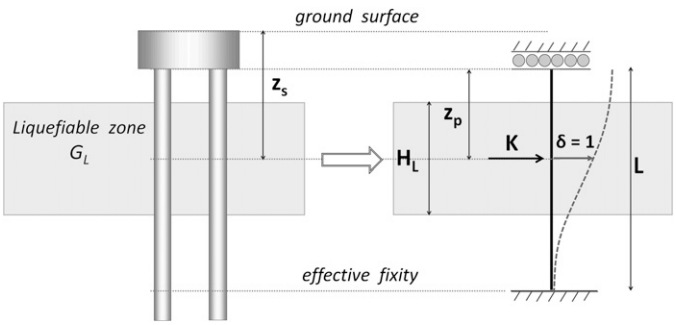

Fig. 5. Illustration of important parameters of the method (described in Table 1)

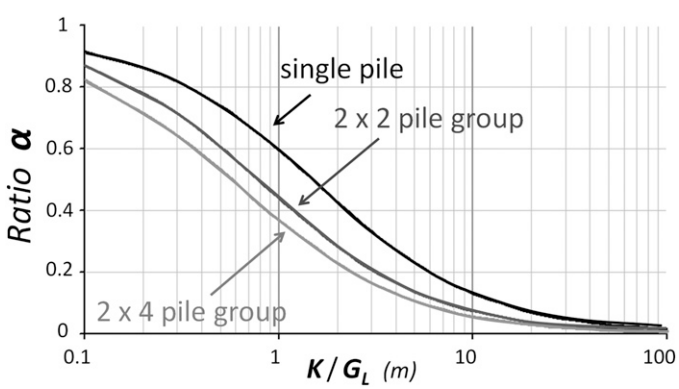

Fig. 6. Ratio α as a function of the relative stiffness between the pile-structure system and the liquefied soil for three different pile configurations: single pile, 2×2, and 2×4 pile group (obtained from several parametric numerical analyses of the horizontal slice)

When the relative stiffness tends to zero ($K/G_L \to 0$), the ratio α tends to unity, which means that the pile slices move just like the soil as rigid inclusions. On the contrary, when the relative stiffness tends to infinity ($K/G_L \to \infty$), the ratio α tends to zero. This is because the soil has insignificant shear strength and flows around the piles without exerting any appreciable load on them. Moreover, Fig. 6 shows that when the number of piles increases, the resistance of the foundation to the moving soil mass becomes stronger. It is worth mentioning that the numerical modeling of the pile group section into the liquefied soil is based on the assumption that as a result of the pile cap constraint, the piles sustain the same horizontal displacement over their entire depth.

Eventually, after producing the ratio α curves for a specific pile configuration and estimating the relative stiffness K/G_L (G_L has been obtained from the first step of analysis), the appropriate ratio α for each case study can be chosen using the graph. Then, the pile displacement at the mid-depth, δ_p, can be calculated by multiplying the selected ratio α with the free-field soil displacement at the mid-depth of the liquefiable zone, δ_{fp}, at the position behind the quay wall to be occupied by the pile group, as obtained from the first step of the analysis. It should be mentioned that the ratio α curves for different pile configurations can be reproduced independently of the first step of analysis.

In the last phase, the total pile deformation at all depths and mainly at the pile top is evaluated. The deformation shape of each pile is controlled primarily by the boundary conditions and only marginally by the load distribution along it. In other words, it can be shown that the shape of the load distribution along the pile (i.e., uniform, p; triangular, 0–p; trapezoidal, 0.5p–1.5p) only slightly affects the response of the pile in terms of displacements, as illustrated in Fig. 7. This observation simplifies the analysis of pile response: a possible idealized load distribution (e.g., trapezoidal) is chosen to be imposed on the pile. Thus, its deformation shape is obtained as a function of the unknown p.

Using the known pile displacement at mid-depth of the liquefiable zone, δ_p (from the second step of the analysis), the shape function of the pile with depth is calibrated, and thus, the unknown

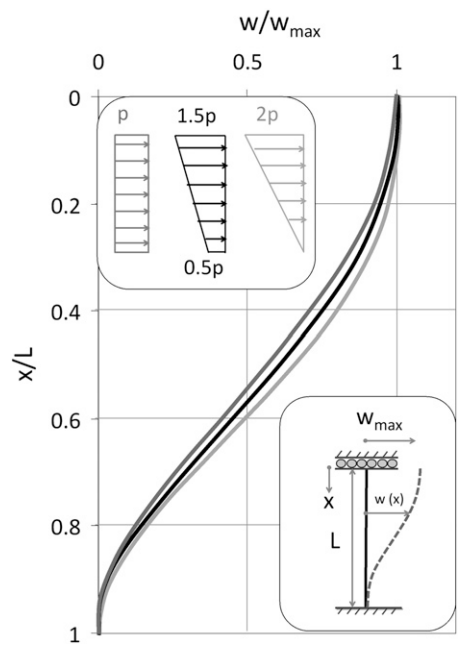

Fig. 7. Pile deflection shapes for three different load distributions (uniform, p; triangular, 0–2p; trapezoidal, 0.5p–1.5p); the pile is fixed at the bottom, and no rotation is allowed at top

J. Geotech. Geoenviron. Eng. 2013.139:223-233.

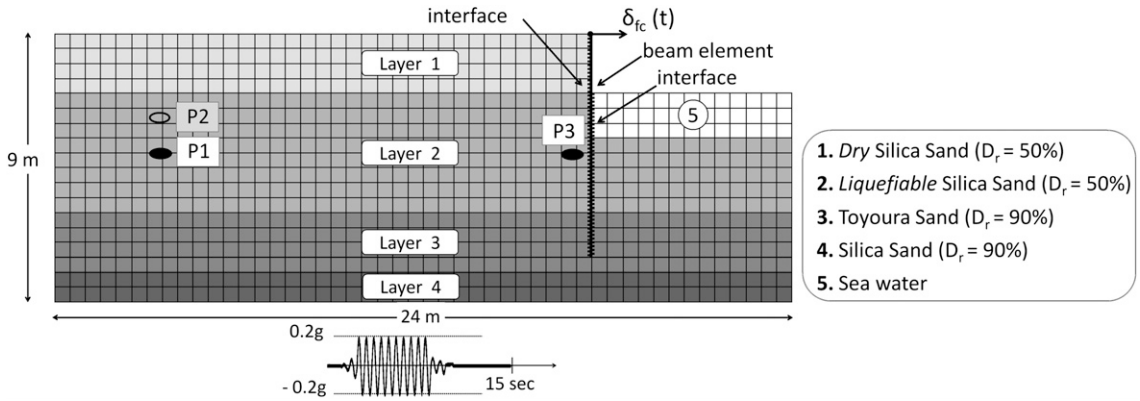

Fig. 8. Numerical Model 1 (first step of the analysis): geometry (in prototype scale), finite-difference discretization in FLAC, and material zones. Points P1 and P3, in the middle of the liquefiable layer, and P2 in its upper quarter recorded the time histories of excess pore pressures

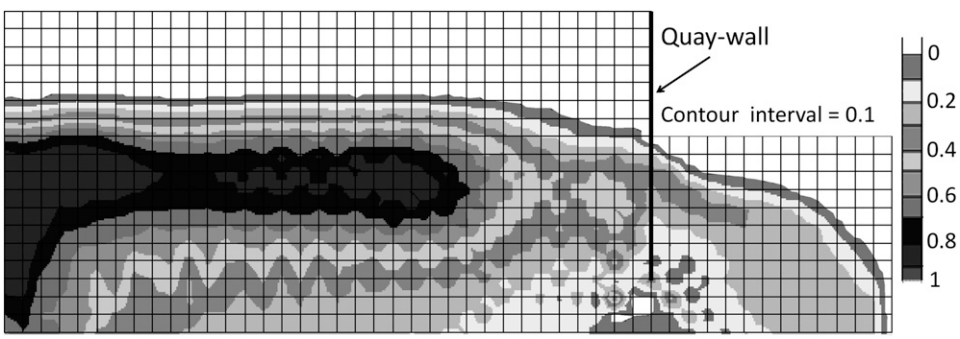

Fig. 9. Numerical Model 1 (first step of the analysis): contours of excess pore pressure ratio (r_u) at $t = 10$ s; liquefaction occurs in the free field away from the quay wall

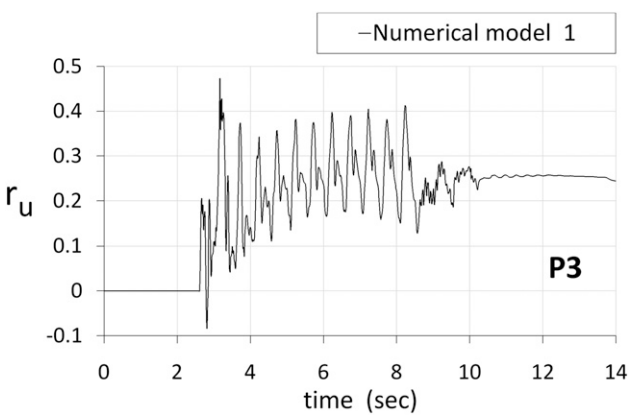

Fig. 10. Numerical Model 1 (first step of the analysis): time history of the (small) excess pore pressure ratio (r_u) computed for Point P3 adjacent to the quay wall

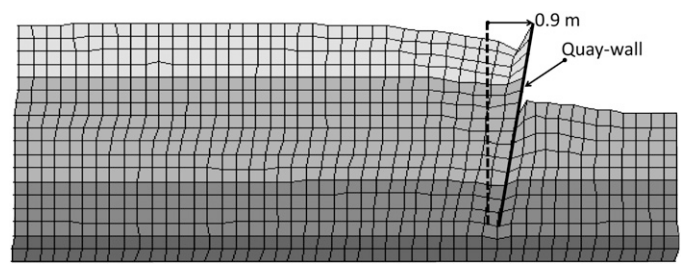

Fig. 11. Numerical Model 1 (first step of the analysis): snapshot of the deformed geometry; the residual horizontal displacement at the top of the quay wall is estimated to be 0.9 m after the end of shaking

load intensity p is estimated. Finally, the distribution of displacements and bending moments along the pile are determined by imposing the already known load distribution on the pile column. The parameters of the method are summarized in the Notation section, and most are illustrated explicitly in Fig. 5.

Validation of the Method: Comparison with Centrifuge Results

According to the first step of the method, a vertical slice of the centrifuge models without the piles is analyzed numerically using the finite-difference code FLAC. The simulation involves the constitutive law of Byrne (1991) for pore-pressure generation, which is incorporated in the standard Mohr-Coulomb plasticity model. Numerical Model 1 simulates exactly Centrifuge Model 1a, and Numerical Model 2 corresponds to Centrifuge Model 2 but without

J. Geotech. Geoenviron. Eng. 2013.139:223-233.

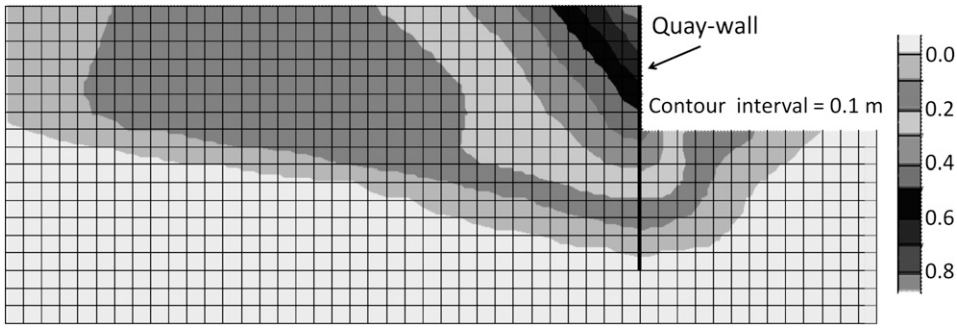

Fig. 12. Numerical Model 1 (first step of the analysis): contours of the horizontal displacements of the quay wall–soil system at $t = 10$ s

the piles. Numerical Model 1 is illustrated in Fig. 8, along with the free-field points (P1, P2, and P3) where time histories of excess pore-pressure ratios are obtained.

The excess pore-pressure ratio, r_u, is defined as the excess pore pressure Δu, over the initial vertical effective stress, σ'_{vo}, given by the following equation:

$$r_u = \frac{\Delta u}{\sigma'_{vo}} \tag{2}$$

In both cases (Numerical Models 1 and 2), liquefaction takes place in the loose sand layer only, away from the quay wall (free field). As indicated by the excess pore-pressure ratio (r_u) contours in Fig. 9 and the corresponding time history next to the quay wall (Point P3) in Fig. 10, excess pore water pressure ratios remain at or below 0.5—obviously as a result of the large outward displacement of the wall that tends to generate negative excess water pressures, reducing the positive ones because of vertical waves (Dakoulas and Gazetas 2005, 2008). This mechanism is reflected in the excess pore-pressure time history (Fig. 10) by the large cyclic component, indicating a sudden increase of r_u when the wall moves inward and sudden dissipation of pore pressures (even reaching negative values) when the wall moves toward the water.

The quay wall sustained a large outward rotation and displacement that, combined with the liquefaction of the free field, induced soil flow (lateral spreading). This response of the quay wall–soil system is clearly portrayed by the deformed grid of Numerical Model 2 after the end of shaking (Fig. 11). The same trend is also shown in Fig. 12, in terms of horizontal displacement contours. The soil displacements decrease with increasing distance from the quay wall, as expected. Based on the fact that Centrifuge Model 1a and Numerical Model 1 are directly comparable (no piles involved in both cases), the comparison of the corresponding results is illustrated in Figs. 13(a and b) in terms of distribution of horizontal soil displacement behind the wall and excess pore-pressure ratio time histories (at Location P1). Both results imply a satisfying agreement related to the evolution of liquefaction and the rate of decrease of horizontal soil displacements as the distance to the waterfront increases. This agreement confirms the validity of numerical modeling.

Liquefaction in the far field has indeed been observed in the centrifuge experiments. Direct quantitative comparison between centrifuge and numerical results has been made only in the case of Centrifuge Model 1a where no piles are involved. Such a comparison cannot be performed for Centrifuge Model 2 because of the presence of piles in the centrifuge and their absence in Numerical Model 2. However, a relatively similar response of the soil is expected away from the piles. In this framework, a comparison between experimental and computed excess pore-pressure ratio time histories in the liquefied layer has been attempted in Fig. 13(c). There is significant agreement between theory and experiment on the rate of buildup of excess pore pressure and on the time of occurrence of liquefaction.

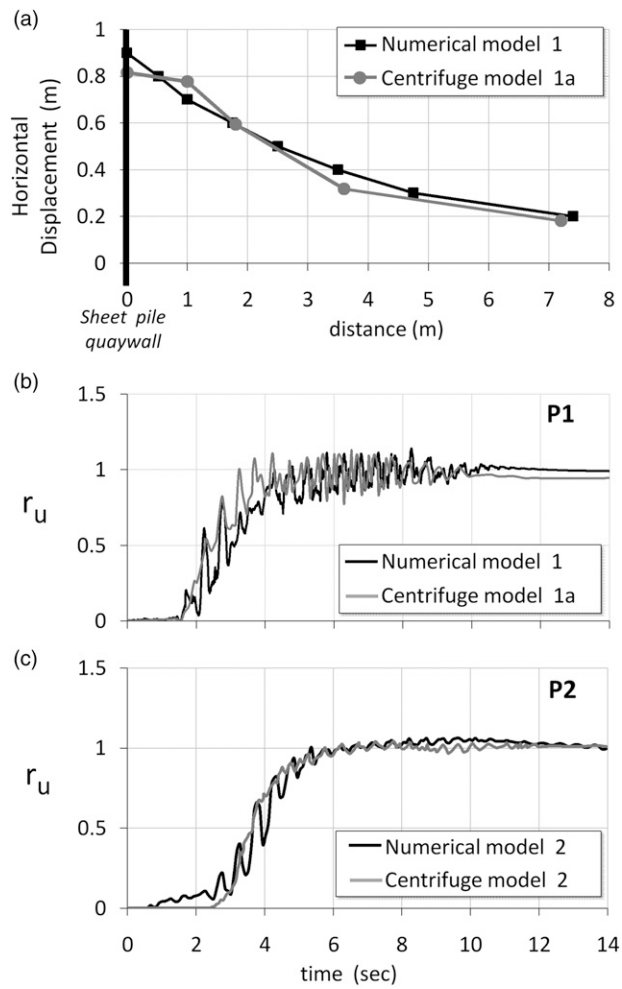

Fig. 13. Comparison between centrifuge and numerical results: (a) distribution of residual horizontal soil displacement versus distance from the quay wall; (b) and (c) time histories of excess pore pressure ratio (r_u) in the free field, obtained from the analysis of Numerical Model 1 at Point P1 and Model 2 at Point P2

Moreover, Figs. 14(a and b) illustrate the computed time histories of the relative horizontal displacement at the top of the quay wall, showing residual values equal to 0.9 and 1.15 m for Models 1 and 2,

J. Geotech. Geoenviron. Eng. 2013.139:223-233.

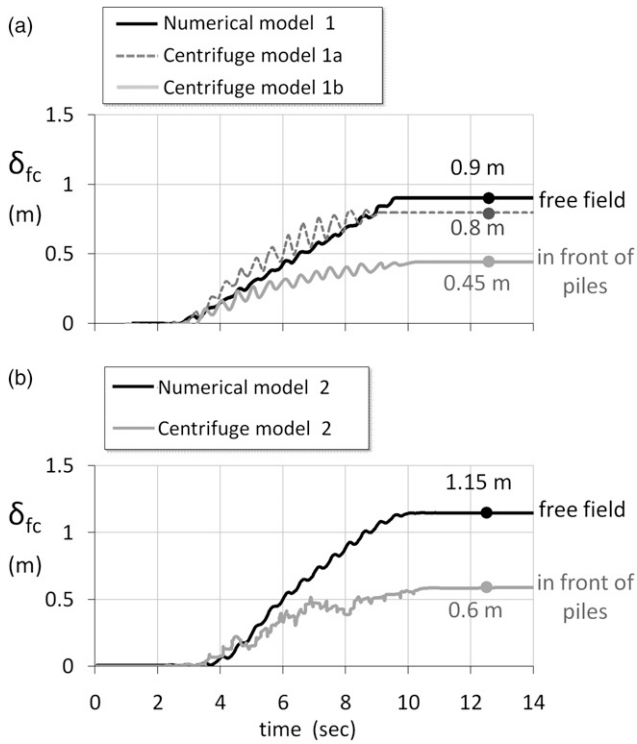

Fig. 14. Comparison of horizontal quay wall displacement (δ_{fc}) time histories between (a) Numerical Model 1 (of first step, no piles), Centrifuge Model 1a (no piles), and Centrifuge Model 1b (with piles) and (b) Numerical Model 2 (of first step, no piles) and Centrifuge Model 2 (with piles)

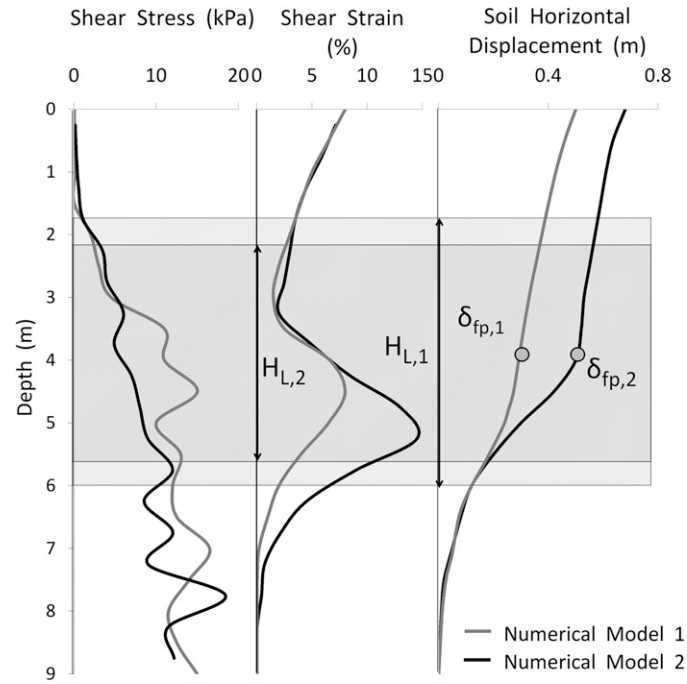

Fig. 15. First step of analysis: computed distribution with depth of residual shear stresses (τ), strains (γ), and horizontal soil displacements, all at the (subsequent) location of the piles, 2.75 and 3 m behind the quay wall for Models 1 and 2, respectively

Table 1. Values Assigned to the Parameters of the Method during Its Application to the Centrifuge Experiments by Tazoh et al. (2005) and Sato et al. (2001)

Parameters of the simplified method		Centrifuge Model 1b (Sato et al. 2001)	Centrifuge Model 2 (Tazoh et al. 2005)
Soil	G_L (kPa)	240	126
	H_L (m)	2.4	3.6
	z_s (m)	3.9	3.9
	δ_{fp} (m)	0.29	0.505
Pile	z_p (m)	2.7	3.3
	EI (kNm^2)	17,000	11,980
	L (m)	7.6	8.1
	K (kN/m)	839	585
Soil-pile interaction	K/G_L (m)	3.5	4.6
	α	0.145	0.146
	δ_p (m)	0.042	0.074
	p_{uniform} (kN/m)	6.46	3.8
	$p_{\text{triangular}}$ (kN/m)	7.3	4.2
	$p_{\text{trapezoidal}}$ (kN/m)	6.86	4

respectively. However, the displacement of the quay wall was approximately 0.45 m in Centrifuge Model 1b and 0.6 m in Centrifuge Model 2, immediately after the end of shaking. That part of this discrepancy stems from the beneficial effect of the presence of the piles in the centrifuge, which inhibits soil movement and reduces wall deflection, as stated by Sato et al. (2001) after quantitative comparison between Centrifuge Models 1a (no piles) and 1b (2×4 pile group).

The distributions of the residual shear stresses (τ) and strains (γ), as well as of the horizontal soil displacements (Fig. 15), are obtained at the location of the hypothetical vertical center line where the pile group will be placed (2.75 and 3 m behind the quay wall for Models 1b and 2, respectively). These distributions are useful when proceeding to the second step, where important parameters of the problem (G_L, δ_{fp}, K/G_L, α, δ_p) are determined. The values of these parameters for each centrifuge experiment are shown in Table 1.

The pile stiffness, K, is estimated given the assumption that each pile in the pile group is equivalent to a beam element fixed at the bottom with no rotation at top. The shear modulus of the liquefied soil, G_L, is computed using Eq. (1). The equivalent shear modulus, G_L, is estimated as 240 kPa for Numerical Model 1 and 126 kPa for Model 2. These values are included in the set of reduced shear modulus values coming from cyclic torsional tests on Toyoura sand specimens to obtain stress-strain curves of liquefied sands at large deformations, published by Yasuda et al. (1995). Alternatively, empirical relationships found in the literature can be chosen to estimate the equivalent shear modulus of liquefied sands, such as the one suggested by Yasuda (2004). The latter relates G_L with the mean initial effective stress, σ'_c, the stress ratio to cause 7.5% of shear strain by 20 cycles of loading, R_L (~0.25 for Toyoura sand), and the safety factor against liquefaction, F_L (0.9–1.0 when the maximum shear strain is about 2–20% for loose sands). This relationship is given by the following equation:

$$G_L = \sigma'_c \alpha e^{\{-\exp[-b(R_L - c)]\}} \tag{3}$$

where

$$\alpha = 23.6F_L + 0.98,$$
$$b = 9.32F_L^3 - 10.8F_L^2 + 13.27F_L - 0.806,$$
$$c = -1.40F_L^3 + 3.87F_L^2 - 4.14F_L + 1.95$$

J. Geotech. Geoenviron. Eng. 2013.139:223-233.

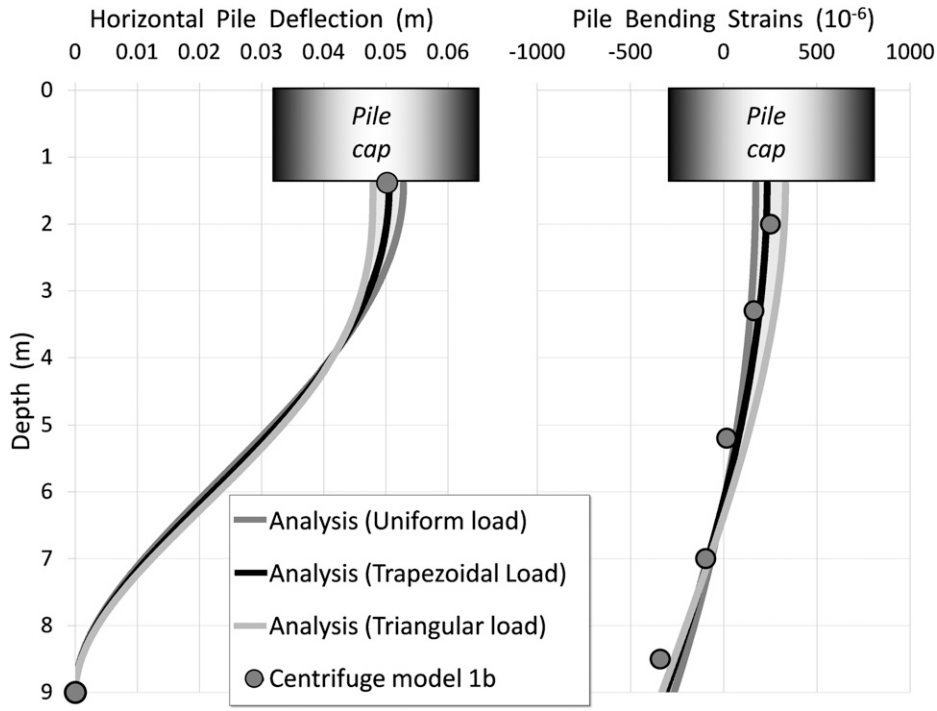

Fig. 16. Computed range of the horizontal deflections and bending strains along the pile, obtained from the simplified method; comparison with the centrifuge data points of Sato et al. (2001)

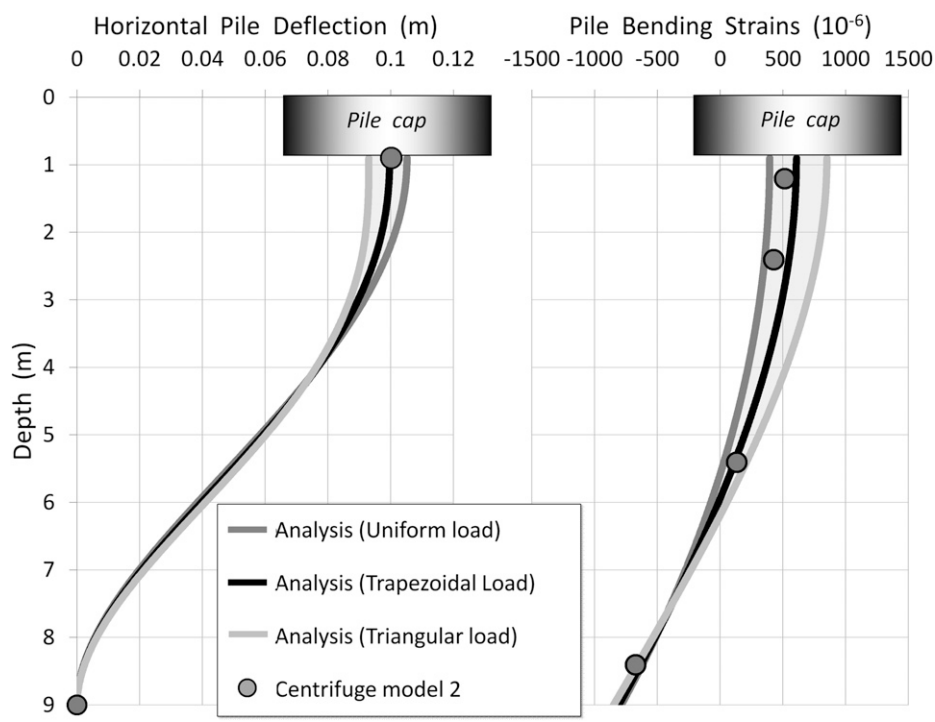

Fig. 17. Computed range of the horizontal deflections and bending strains along the pile, obtained from the simplified method; comparison with the centrifuge data points of Tazoh et al. (2005)

According to Eq. (3), the reduced shear modulus, G_L, obtains values in the range of 94–245 kPa, for $\sigma_c' = 40$ kPa at the mid-depth of the liquefiable zone, $R_L = 0.25$, and $F_L = 0.9-1.0$. It is obvious that both values of G_L predicted by Eq. (1) (240 kPa for Model 1 and 126 kPa for Model 2) fall into this range.

Another way to estimate the reduction of initial shear modulus caused by pore-pressure generation is to use the G-γ curves for saturated sands suggested in the literature, such as the one proposed by Hardin and Drnevich (1972a, b). According to the definition of G_L here by Eq. (1), the ratio where G_o is the initial shear modulus, is

J. Geotech. Geoenviron. Eng. 2013.139:223-233.

estimated to be 0.0087 for an average maximum shear strain, γ, equal to 4% within the liquefied layer (Fig. 15) and 0.0045 for γ equal to 7% in the cases of Models 1 and 2, respectively. These pairs of $(G_L/G_o, \gamma)$ are in good agreement with the aforementioned G-γ curve by Hardin and Drnevich (1972a, b).

The relative stiffness, K/G_L, is thus known, and the ratio α is subsequently determined appropriately for each case (2×2 and 2×4 pile groups) according to the graph in Fig. 6. The pile displacement at mid-depth of the liquefiable layer, δ_p, is estimated as the product of the ratio α and the soil displacement at the same depth, δ_{fp}, obtained from the first step (shown clearly in Fig. 15).

Proceeding to the final phase, aiming to obtain estimates of the distributions of horizontal displacements and bending strains, three different load distributions (uniform, triangular, and trapezoidal) of yet unknown intensity p are imposed on the pile-beam element. Thus, the deformation line of the pile is initially formed as a function of p, which can be specified using one known point of the pile displacement at the mid-depth of the liquefied zone (z_p, δ_p). Then, the bending strains along the pile are obtained through double differentiation of the displacements. Thus, computed displacements and bending strain distribution are depicted in Figs. 16 and 17 and compared with the experimental recordings. The agreement is satisfactory. In particular, the trapezoidal distribution seems to give the most accurate prediction of both displacements and strains.

Concluding Remarks

In this paper, a simple physically motivated method of analysis is highlighted for the evaluation of pile response caused by liquefaction-induced soil flow. The method has been validated by means of comparison with centrifuge results. The two characteristic attributes of the method are as follows:

- It avoids the associated empirical selection of stiffness-reduction factors and does not involve the use of p-y curves; and
- It combines the results of analysis of a vertical two-dimensional (2D) section of the geometry without the presence of piles and of the pseudo-static analysis of a horizontal 2D slice containing the piles. Interaction between soil and piles is determined as a function of the relative stiffness between the pile-superstructure system and the liquefied soil.

The method, in combination with suitable engineering judgment and reasonable assumptions, can provide sufficient accuracy for designing pile groups against liquefaction-induced large soil displacements.

Acknowledgments

Financial support for this paper was provided under the research project, DARE, which is funded through the IDEAS Programme of the European Research Council's (ERC), in support of frontier research, under Contract No. ERC-2-9-AdG228254-DARE.

Notation

The following symbols are used in this paper:

G_L = shear modulus of liquefied soil;
H_L = thickness of liquefied zone;
K = horizontal stiffness of the pile column at the mid-depth of liquefied zone;
L = active length of the pile;
p = load value describing the potential load distribution along the pile;
z_p = mid-depth of liquefied zone measured from the top of the pile;
z_s = mid-depth of liquefied zone measured from the ground surface;
α = ratio of horizontal pile displacement over horizontal soil displacement at the mid-depth (z_s) in the free field;
δ_{fp} = free-field horizontal soil displacement at the mid-depth of liquefied zone and at the location potentially occupied by the pile foundation; and
δ_p = pile displacement at mid-depth of the liquefied layer, z^s.

References

Berrill, J. B., and Yasuda, S. (2002). "Liquefaction and piled foundations: Some issues." *J. Earthquake Eng.*, 1(6), 1–41.

Boulanger, R. W., Kutter, B. L., Brandenberg, S. J., Singh, P., and Chang, P. (2003). "Pile foundations in liquefied and laterally spreading ground during earthquakes: Centrifuge experiments and analyses." *Rep. No. UCD/CGM-03/01*, Dept. of Civil and Environmental Engineering, Univ. of California, Davis, CA.

Budek, A. M., Priestley, M. J. N., and Benzoni, G. (2000). "Inelastic seismic response of bridge drilled-shaft RC pile/columns." *J. Geotech. Geoenviron. Eng.*, 126(4), 510–517.

Byrne, P. (1991). "A cyclic shear-volume coupling and pore-pressure model for sand." *Proc., 2nd Int. Conf. on Recent Advances in Geotechnical Earthquake Engineering and Soil Dynamics,* S. Prakash, ed., Univ. of Missouri–Rolla, Rolla, MO, 47–55.

Caltrans. (1990). *Bridge design specifications/seismic design references*, Caltrans, Sacramento, CA.

Cubrinovski, M., and Ishihara, K. (2004). "Simplified method for analysis of piles undergoing lateral spreading of liquefied soils." *Soil Found.*, 44(5), 119–133.

Cubrinovski, M., Kokusho, T., and Ishihara, K. (2006). "Interpretation from large-scale shake table tests on piles undergoing lateral spreading in liquefied soils." *Soil Dyn. Earthquake Eng.*, 26(2), 275–286.

Dakoulas, P., and Gazetas, G. (2005). "Seismic effective-stress analysis of caisson quay walls: Application to Kobe." *Soil Found.*, 45(4), 133–147.

Dakoulas, P., and Gazetas, G. (2008). "Insight to seismic earth and water pressures against caisson quay walls." *Geotechnique*, 58(2), 95–111.

Dobry, R., and Abdoun, T. H. (2001), "Recent studies on seismic centrifuge modeling of liquefaction and its effect on deep foundations." *Proc., 4th Int. Conf. on Recent Advances in Geotechnical Earthquake Engineering and Soil Dynamics Symposium,* S. Prakash, ed., Vol. 2, Univ. of Missouri–Rolla, Rolla, MO.

Dobry, R., Abdoun, T., O'Rourke, T. D., and Goh, S. H. (2003). "Single piles in lateral spreads: Field bending moment evaluation." *J. Geotech. Geoenviron. Eng.*, 129(10), 879–889.

Finn, W. D. L., and Fujita, N. (2002). "Piles in liquefiable soils: Seismic analysis and design issues." *Soil. Dyn. Earthquake Eng.*, 22 (9–12), 731–742.

Hamada, M. (2000). "Performances of foundations against liquefaction-induced permanent ground displacements." *Proc., 12th World Conf. on Earthquake Engineering*, New Zealand Society for Earthquake Engineering, Silverstream, New Zealand, 1754–1761.

Hardin, B. O., and Drnevich, V. P. (1972a). "Shear modulus and damping in soils: Design equations and curves." *J. Soil Mech. Found. Div.*, 98(7), 667–692.

Hardin, B. O., and Drnevich, V. P. (1972b). "Shear modulus and damping in soils: Measurement and parameter effects." *J. Soil Mech. Found. Div.*, 98(6), 603–624.

Itasca Consulting Group. (2005). *Fast Lagrangian analysis of continua,* Itasca Consulting Group, Minneapolis.

Japan Road Association (JRA). (1996). *Specification for highway bridges*, Japan Road Association, Tokyo (in Japanese).

J. Geotech. Geoenviron. Eng. 2013.139:223-233.

Priestley, M. J. N., Seible, F., and Calvi, G. M. (1996). *Seismic design and retrofit of bridges*, Wiley, New York.

Sato, M., Tazoh, T., and Ogasawara, M. (2001). "Reproduction of lateral ground displacement and lateral flow—Earth pressure acting on pile foundations using centrifuge modeling." *Proc., 4th Int. Conf. on Recent Advances in Geotechnical Earthquake Engineering and Soil Dynamics Symposium,* S. Prakash, ed., Univ. of Missouri–Rolla, Rolla, MO.

Tazoh, T., Sato, M., and Gazetas, G. (2005). "Centrifuge tests on pile–foundation−structure systems affected by liquefaction-induced soil flow after quay wall failure." *Proc., 1st Greece–Japan Workshop: Seismic Design, Observation, and Retrofit of Foundations*, G. Gazetas and T. Tazoh, eds., Laboratory of Soil Mechanics, National Technical Univ. of Athens, Athens, Greece, 79–106.

Tokimatsu, K., and Asaka, Y. (1998). "Effects of liquefaction-induced ground displacements on pile performance in the 1995 Hyogoken-Nambu earthquake." *Soil Found.*, 1998(Special Issue), 163–177.

Tokimatsu, K., Mizuno, H., and Kakurai, M. (1996). "Building damage associated with geotechnical problems." *Soil Found.*, 1(Special Issue), 219–234.

Wood, D. M. (2004). *Geotechnical modelling*, Cambridge University Press, Cambridge, U.K.

Yasuda, S. (2004). "Evaluation of liquefaction-induced deformation of structures. Recent advances in earthquake geotechnical engineering and microzonation." *Geotech. Geol. Earthquake Eng.*, 1, 199–230.

Yasuda, S., Abo, H., Yoshida, N., Kiku, H., and Uda, M. (2001). "Analyses of liquefaction-induced deformation of grounds and structures by a simple method." *Proc., 4th Int. Conf. on Recent Advances in Geotechnical Earthquake Engineering and Soil Dynamics Symposium*, S. Prakash, ed., Univ. of Missouri–Rolla, Rolla, MO.

Yasuda, S., Yoshida, N., Masuda, T., Nagase, H., Mine, K., and Kiku, H. (1995). "Stress–strain relationships of liquefied sands." *Proc., 1st Int. Conf. on Earthquake Geotechnical Engineering*, K. Ishihara, ed., A. A. Balkema, Rotterdam, Netherlands, 811–816.

J. Geotech. Geoenviron. Eng. 2013.139:223-233.